Permafrost thaw in a nested groundwater-flow system

Jeffrey M. McKenzie · Clifford I. Voss

Abstract Groundwater flow in cold regions containing permafrost accelerates climate-warming-driven thaw and changes thaw patterns. Simulation analyses of groundwater flow and heat transport with freeze/thaw in typical cold-regions terrain with nested flow indicate that early thaw rate is particularly enhanced by flow, the time when adverse environmental impacts of climate-warming-induced permafrost loss may be severest. For the slowest climate-warming rate predicted by the Intergovernmental Panel on Climate Change (IPCC), once significant groundwater flow begins, thick permafrost layers can vanish in several hundred years, but survive over 1,000 years where flow is minimal. Large-scale thaw depends mostly on the balance of heat advection and conduction in the supra-permafrost zone. Surface-water bodies underlain by open taliks allow slow sub-permafrost flow, with lesser influence on regional thaw. Advection dominance over conduction depends on permeability and topography. Groundwater flow around permafrost and flow through permafrost impact thaw differently; the latter enhances early thaw rate. Air-temperature seasonality also increases early thaw. Hydrogeologic heterogeneity and topography strongly affect thaw rates/patterns. Permafrost controls the groundwater/surface-water-geomorphology system; hence, prediction and mitigation of impacts of thaw on ecology, chemical exports and infrastructure require improved hydrogeology/permafrost characterization and understanding.

Keywords Cold regions hydrology · Permafrost · Regional flow · Groundwater modeling · Cryology

Received: 11 July 2012 / Accepted: 21 November 2012

Published in the theme issue "Hydrogeology of Cold Regions"

J. M. McKenzie (✉)
Earth and Planetary Sciences,
McGill University, Montreal, Quebec H3A 0E8, Canada
e-mail: jeffrey.mckenzie@mcgill.ca
Tel.: +1-514-3983833

C. I. Voss
US Geological Survey, Menlo Park, CA 94025, USA
e-mail: cvoss@usgs.gov

Introduction

Arctic hydrologic systems are particularly sensitive to a warming climate due to the existence of perennially frozen ground (permafrost) in these regions. Arctic hydrology has been reportedly undergoing rapid changes, perhaps as a result of short- or long-term climate change, as observed by increased carbon export in Eurasian arctic rivers, increases in arctic river discharge, and disappearance of arctic lakes (White et al. 2007). Permafrost in these regions ranges in thickness from several meters to hundreds of meters and it is an effective barrier to groundwater flow. It impedes recharge and discharge and blocks groundwater flow in the unfrozen region below the permafrost. As permafrost thaws from above in a warming climate, a deeper seasonal active zone (the shallow supra-permafrost subsurface layer that freezes and thaws annually) develops and also more through-going thawed zones (i.e. open taliks) gradually develop, connecting the supra- and sub-permafrost zones. Unfrozen pathways above, within, below and through permafrost can allow a dramatic increase of interaction between groundwater and surface water. Further, where groundwater flow is significant, it can impact the rate and pattern of thaw via heat advection in relatively warm supra-permafrost recharge water and sub-permafrost geothermally warmed water. Accelerated thaw further increases groundwater flow, creating a 'feedback' mechanism, in which increased groundwater flow begets even more groundwater flow. Despite the potential for increasing groundwater flux in warming arctic environments, until recently (McKenzie et al. 2007; Bense et al. 2009; Frampton et al. 2011; Ge et al. 2011; Painter 2011; Rowland et al. 2011; Bense et al. 2012; Wellman et al. 2012, in this issue), predictive models of permafrost thaw and distribution generally considered only the conduction of heat through the subsurface, and did not incorporate advective heat transport (migration of energy due to groundwater flow). Where heat advection is dominant (Kane et al. 2001), neglect of advection in favor of conduction in analyses of cold regions hydrology would result in significantly different predicted evolution of the timing and spatial pattern of thaw for a warming climate, with concomitant differences in prediction of impacts on surface waters, chemical exports and ecosystems.

To provide a tool with which to develop understanding of the groundwater-ground ice system and potential feedbacks, the US Geological Survey's SUTRA groundwater simulator (Voss and Provost 2002) coupling groundwater flow and

DOI 10.1007/s10040-012-0942-3

Published online: 17 January 2013

heat transport, was modified to include the water freeze/thaw process (McKenzie et al. 2007). For sub-zero temperatures in the subsurface, the modified computer code accounts for time-variations in liquid/ice saturations, permeability and thermal properties, and it includes the latent heat of freeze/thaw in its energy balance.

In order to investigate the interplay of heat conduction and heat advection via groundwater flow with both seasonal ground ice and permafrost in arctic hydrologic systems, an idealized typical cold-regions terrain is modeled in the present study with the modified SUTRA code. The region represents an area with undulating topography reminiscent of the type analyzed in the classical work of Toth (1963), in which the existence of and controls on nested three-dimensional (3D) groundwater flow patterns were first quantitatively described. For a similar terrain and within a set of nested groundwater flow systems, the present study evaluates the impacts of a key (though not exhaustive) set of surface and hydrogeologic controls on the timing and pattern of permafrost thaw during climate warming. The controls considered are:

- Frequency and amplitude of topographic (i.e. water table) undulation
- Permeability value ('zero' permeability giving conduction-only heat transport, and also a range of low to high realistic values)
- Vertical anisotropy in permeability (ratio of horizontal to vertical permeability, ranging from no anisotropy to high values representing the upscaled effect of low-permeability layers)
- Heterogeneity in spatial distribution of permeability (patchiness consisting of high- and low-permeability structures)
- Lakes/streams in valleys with perennially unfrozen bottom water (none, one, or more water bodies)
- Initial permafrost state (permafrost initially much colder than thaw temperature range, and, permafrost initially ready to thaw with only minor temperature increase)
- Extent of groundwater flow through permafrost body (no throughflow, and, some throughflow)
- Climate-warming rate (low and high estimates)
- Amplitude of seasonal temperature variation (none and a range from low to high) superimposed on a linear temperature trend representing a warming climate

This study is not intended to be comprehensive regarding behavior of ground ice in groundwater flow settings; rather, it is intended to identify some of the most important processes and phenomena that warrant further study.

Approach

Freeze/thaw simulation details

Groundwater flow with conductive-advective energy transport and with freezing and thawing of groundwater is simulated with a modified version of the SUTRA computer code (McKenzie et al. 2007). In the current study, only saturated groundwater conditions are considered; thus, pores are fully filled with some proportion of ice and liquid water, depending on temperature. A variety of functional forms for the fraction of liquid water as a function of temperature are possible, but for simplicity in the current analysis, a linear form is employed in which freezing begins when temperature drops to 0 °C, and the fraction of ice increases linearly with decreasing temperature until a maximum ice fraction of 0.99 and residual liquid-water fraction of 0.01 (i.e. 1 % of the pore volume is liquid, 99 % is ice) occurs at −2 °C. For temperatures colder than −2 °C, the liquid saturation remains at the residual value. In general, groundwater flow occurs in ice-free regions of the subsurface, and flow is also possible through partially frozen regions (where the ice fraction is between zero and its maximum value). In this regard, another simplification is introduced in order to clearly illustrate the impact on ground-ice state and evolution of exclusively the groundwater flow that occurs in ice-free parts of the subsurface, in contrast with the flow that may occur through partially frozen permafrost. In the present analysis for most cases considered, wherever ice forms, even for very low ice saturation values, permeability is lowered by a factor of 10^6 from its unfrozen value. In the other cases, some groundwater flow is allowed to flow through permafrost, to evaluate the additional impact of this process on thaw. Other thermal properties, used for all simulations, are given in Table 1.

The McKenzie et al. (2007) modifications to the SUTRA code employed a linear relation between fluid density and temperature. In the present work, a nonlinear function is implemented in the form of the empirical Thiesen-Scheel-Diesselhorst (TSD) equation (Tilton and Taylor 1937; Kell 1967). The liquid water density, ρ, is nonlinearly dependent on temperature, T, as follows (Fig. 1):

$$\rho = 1000\left[1 - \frac{(T + 288.9414)(T - 3.9263)^2}{508929.2(T + 68.12063)}\right]$$

For small ranges of temperature around 0 °C, density effects on fluid flow are expected to be small, due to the near constancy of density values; however, for ranges that are larger and typical of the present study (−16 °C mid-winter air temperature to 40 °C temperature at 2 km depth), fluid density differences (approx. 995 kg/m^3 at the extremes to a maximum of 1,000 kg/m^3 at 2 °C) are sufficient to drive flow when permeability values are sufficiently high, and circulations are sometimes observed in the simulated regions below permafrost. The density of ice is assumed to be constant, regardless of temperature (Table 1).

Model domain, mesh, and boundary conditions

The two-dimensional (2D) cross-sectional model domain is reminiscent of 'Tothian hills' in the spirit of the classic

DOI 10.1007/s10040-012-0942-3

Table 1 Parameters used in freeze/thaw simulations

Parameter	Value
Ice	
Ice specific heat (J/kg)	2,108
Ice thermal conductivity [J/(sm°C)]	2.14
Density of ice (kg/m^3)	920
Latent heat of fusion (J/kg)	334,000
Liquid water	
Fluid specific heat (J/kg)	4,182
Fluid thermal conductivity [J/(sm°C)]	0.6
Fluid compressibility [kg/(ms^2)]$^{-1}$	4.47×10^{-10}
Solid matrix	
Solid grain specific heat (J/kg)	840
Solid grain thermal conductivity [J/(sm°C)]	3.5
Solid matrix compressibility [kg/(ms^2)]$^{-1}$	1×10^{-8}
Density of solid grains (kg/m^3)	2,600
Porosity (−)	0.1
Other	
Gravity (m/s^2)	−9.81
Longitudinal dispersivity	0.5
Transverse dispersivity	0.5
Freezing function	
Type	Linear
Minimum liquid saturation (−)	0.01
Temperature at which minimum liquid saturation occurs (°C)	−2.0
Permeability of frozen regions, irrespective of ice saturation (m^2)	10^{-40}
Boundary layer above ground surface	
Heat transfer coefficient (defined via settings given below) [J/(sm^2°C)]	1.25
Height (m)	1
Freezing function	None
Permeability (m^2)	10^{-40}
Specific heat (J/kg)	0
Solid grain thermal conductivity [J/(sm°C)]	1.25
Porosity (−)	Top=$1.\times10^{-5}$ bottom=0.1
Bottom boundary geothermal energy flux	
Energy source [(J/s)/m^2]	0.085

analysis of Toth (1963). The ground surface is the assumed location of the water table. The top of the domain represents a location 1 m above the ground surface. The uppermost 1 m of the domain is used to explicitly model heat transfer through an equivalent thermal boundary layer that represents the roughness of ground surface, vegetation and snow pack, as described in the following section. The mean ground surface elevation

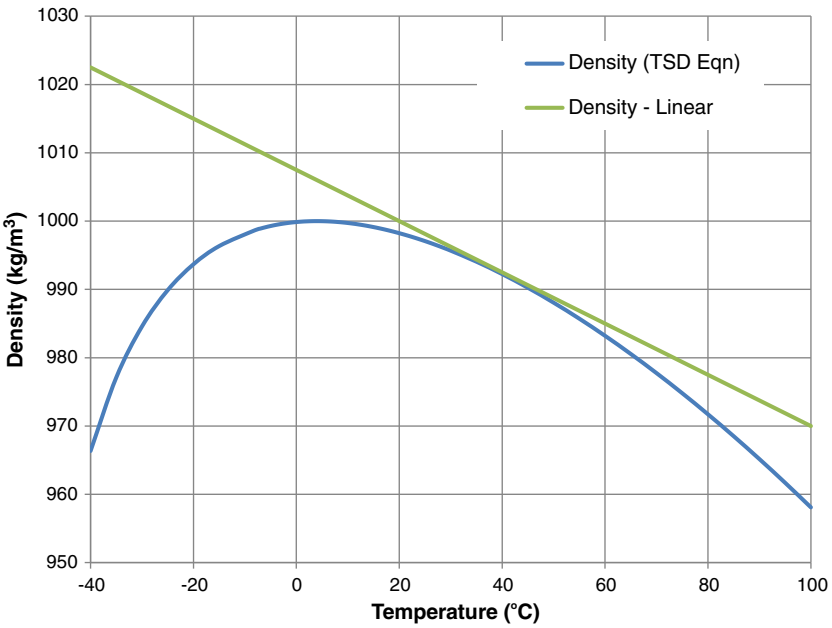

Fig. 1 Fluid density as a function of temperature. Comparison of linear and nonlinear (Thiesen-Scheel-Diesselhorst, *TSD*) functions

DOI 10.1007/s10040-012-0942-3

of the domain rises linearly from left to right, with a single uniform slope. Sinusoidal hills of uniform frequency and amplitude are superimposed on the sloping surface, following the approach of Toth (1963). Figure 2 illustrates the overall extent of the domain (5 km length, approximately 2 km depth) for one example of topographic undulation superimposed on the linearly increasing mean ground-surface elevation. The same value of the mean slope (20 m/km) is used for all analyses. The cross-sectional model is 1 m in thickness. The finite-element mesh is also shown in Fig. 2. Depending on the topographic shape and permeability values, a nested combination of local flow systems (one below each hill) and a larger-scale domain-wide flow system (driven by the regional slope) may exist in the domain. Spatial discretization consists of 1 m × 50 m finite elements in the top (finest) band of elements, 10 m × 50 m in the middle band, and approximately 50 m × 50 m in the deepest band. For some simulations with high permeability or heterogeneous permeability, a finer discretization is employed (as little as 0.5-m vertical spacing in the upper band of elements).

The shape of the top of the model domain is similar to that implied by Toth's sinusoidal hills, but in the Toth analysis, the actual shape of the domain was a perfect rectangle and only the applied values of pressure along the top boundary condition varied sinusoidally with lateral distance. In the present analysis, the actual height of the domain top boundary, Z, undulates and is defined by the following function:

$$Z(x) = z_o + x\tan(\alpha) + h\cos\left(\frac{2\pi x}{\lambda} + \pi\right)$$

$Z(x)$ is the elevation of the top surface as a function of the distance, x, from the left boundary of the domain. z_o is the reference elevation at the left side of the domain, α is the slope of the incline, h is the amplitude of hill height, and λ is the length of each hill-valley combination (wavelength). For the domain shown in Fig. 2, z_o is 2,000 m, h is 50 m, α is 0.02 and λ is 2,000 m.

Boundary conditions

Boundary conditions for the fluid mass balance (groundwater flow model) are as follows. A no-flow condition is specified along the bottom and vertical sides of the domain. A specified pressure boundary condition with a pressure of 0 Pa, representing atmospheric pressure, is specified all along the top of the domain, but at a depth of 1 m below the top (i.e. just below the thermal boundary layer). This boundary condition allows water to freely enter (groundwater recharge) and exit (groundwater discharge) the model domain wherever possible when ice below does not block entry or exit.

Boundary conditions for the energy balance (heat transport model) are as follows. A no-flux (insulated) condition is specified along the vertical sides of the domain. Along the bottom, a heat source of 0.085 J/(sm^2) is specified, equivalent to the heat flux that occurs for a typical vertical lapse rate of 26.5 °C/km when a typical thermal conductivity of geologic fabrics of 3.21 J/(sm°C) is employed in the model.

A specified temperature boundary condition (Fig. 2), with a time-varying temperature value representing air temperature, is specified all along the top of the domain on the upper surface of the thermal boundary layer. The thermal boundary layer represents the physics of a steady heat conduction process (with linear temperature change across the layer) through any insulators that separate the air from the water table. The unit-thickness boundary layer has negligible permeability to avoid flow (10^{-40}m^2), zero heat capacity to enforce steady heat transport conditions, and a thermal conductivity of 1.25 (W/m°C) to represent the heat transfer coefficient, which is representative of conditions in northern Minnesota, USA

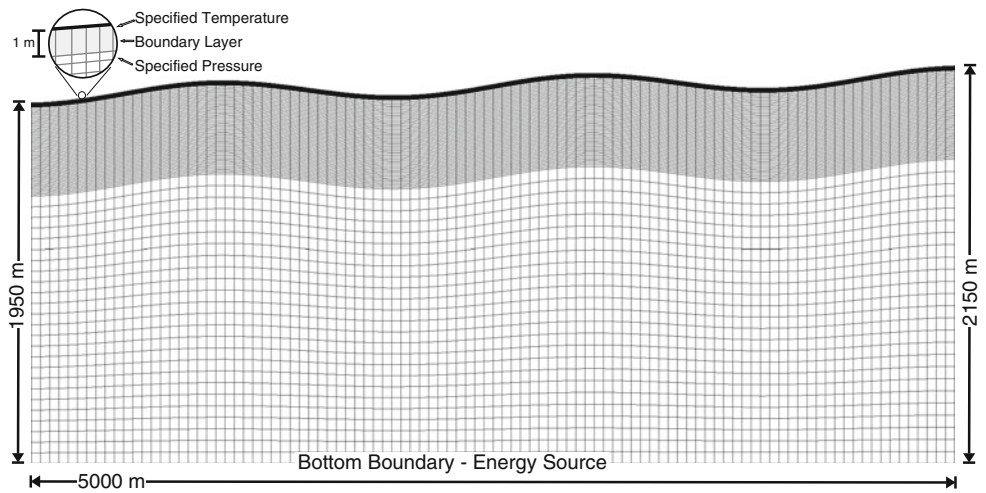

Fig. 2 'Tothian Hills' model domain (no vertical exaggeration) for reference topographic shape with finite-element mesh (coarsest of several used for simulations) and boundary conditions. The mean slope (without the superimposed sinusoidal topography) is 20 m/km. Discretization for this mesh: uppermost 26 m (element thickness, 1 m), below subsequent 480 m (element thickness, 10 m), bottom 1,445–1,645 m (element thickness, 57.8–65.8 m). Model parameters are given in Table 1

 DOI 10.1007/s10040-012-0942-3

(McKenzie et al. 2006). This top boundary condition allows heat to freely be transferred into or out of the subsurface. During times when frozen ground blocks recharge and discharge of groundwater, the only thermal connection of subsurface temperature to atmospheric temperature is via this boundary condition—i.e. conduction-like heat transfer through the thermal boundary layer. During this period, the ground surface temperature tends to be warmer than the air temperature. For ice-free conditions, water can recharge and discharge; during these periods, total heat transport (conduction plus advection) into and out of the subsurface is typically dominated by advection. Water that enters the subsurface due to the specified pressure boundary condition, discussed in the preceding, has a temperature equal to the current atmospheric temperature. Water that discharges from the subsurface at a location of specified pressure has the temperature of the subsurface, which may be colder or warmer than current air temperature.

Air temperature and warming

A general function is specified for air temperature, allowing simulation of a constant or linear increase in mean yearly air temperature with time, or additionally with a superimposed sinusoidal seasonal variation. This air-temperature function, with increasing mean air temperature, is applied to all simulations in this study. At a given time, t (in years), the air temperature, T_{Air} (in degrees C), is calculated as:

$$T_{\mathrm{Air}} = T_{\mathrm{Initial}} + T_{\mathrm{Slope}}\, t + T_{\mathrm{Amplitude}}\, sin(2\pi t)$$

where the angle of the sin is in radians, T_{Initial} (°C) is the starting temperature, T_{Slope} (°C) is the change in mean annual air temperature per year, and $T_{\mathrm{Amplitude}}$ (°C) is the amplitude of yearly air temperature variation (i.e. half of the difference between maximum and minimum temperature in each 1-yearcycle).

For all analyses (except one considering initially warmer permafrost), the initial atmospheric temperature is −6 °C and the increase of mean annual air temperature is either +1 or +6 °C/100 yr. These rates of increase bracket the very low end and very high end of the IPCC (2007) warming prediction range. The amplitudes of the yearly temperature variations considered are ±5, ±10, ±15 and ±20 °C. One variation considers a higher initial atmospheric temperature of −3 °C, to assess the differences in thaw evolution of initially colder vs. warmer permafrost.

Definition of elapsed time for thawing

For simulations with yearly temperature variation, thawing can occur in the summer even when the mean yearly temperature is negative, and freezing can occur in the winter even when the mean yearly temperature is positive, as is the case even in more-temperate climates. For simulations with no seasonal temperature variation, the supra-permafrost thawed zone begins to form once the air temperature becomes greater than 0 °C. This point occurs after 600 and 100 years of simulation for the two rates of increase considered. In order to organize and compare results, elapsed thaw times for all cases reported here are from the time when the annual average air temperature reaches 0 °C. As groundwater flow in most cases considered here (those with no yearly air-temperature fluctuation and those with no groundwater flow through permafrost) can occur only after this point in time, this selection of a reference time allows comparison of the impact of groundwater flow on thaw evolution for a variety of scenarios.

Discretization in time

Time step size is held constant throughout each simulation at a value adjusted for efficiency in simulation time while preserving numerical stability during the nonlinear freeze/thaw periods. Time step size is less than or equal to 0.05 years for all simulations based on numerical convergence tests with smaller time step sizes. Numerical tests show that no iterations to resolve nonlinearity are required (one iteration per time step is employed).

Hydrogeology

Hydrogeology is treated simply with the objective of capturing the effect of hydrogeologic parameters and patterns on the thaw processes being simulated. In most cases considered, uniform homogeneous representations of geologic fabrics are employed, parameterized by values of horizontal and vertical permeability and porosity. Additionally, some layered and patchy heterogeneous lithologic patterns are considered. Permafrost thaw evolution in a range of possible geologic fabrics that would host a range of potential groundwater flows, from negligible (clay-loess-silt) to relatively high (silty sand, clean fine sand, clean coarse sand), are evaluated. A range of horizontal permeabilities as low as $10^{-40}\mathrm{m}^2$ and from 10^{-15} to $10^{-10}\mathrm{m}^2$ (approximately equivalent to hydraulic conductivities of, respectively, 10^{-33}m/s and 10^{-8} to 10^{-3} m/s) is considered. A range of vertical permeabilities as low as $10^{-40}\mathrm{m}^2$ and from 10^{-16} to $10^{-10}\mathrm{m}^2$ is considered, providing a range of vertical anisotropy in permeability (ratio of horizontal permeability to vertical permeability) of 1 to 1,000, representing different degrees of lithologic stratification. For simplicity, the water table is assumed to be, at all times, coincident with the ground-surface topography. This assumption inflates the quantity of groundwater recharge, particularly in cases with more-permeable aquifer fabrics and with greater topographic slopes. More realistically, the water table in some locations would drop below the ground surface seasonally or perennially, as a result of insufficient availability of snowmelt, rainfall or other sources of recharge to keep it sufficiently elevated. Thus, when evaluated in this simple manner, simulated groundwater flux is considered to be

 DOI 10.1007/s10040-012-0942-3

the maximum possible flux, and its impact on thaw evolution is considered as the maximum possible impact of groundwater flow, for each hydrogeologic case considered.

Initial conditions

For simulations of permafrost thaw during climate warming, an initial distribution of permafrost is required. Although different hydrogeologic conditions might imply a different initial permafrost distribution, for most of the cases simulated here, the same initial permafrost distribution is used so that differences in thaw evolution will be the result of only processes that occur during the warming period. With this approach, controls on permafrost evolution can be most-clearly elucidated. The simplest initial permafrost distribution is obtained for a system dominated by heat conduction with a constant sub-zero air temperature.

Initial conditions are specified in terms of both a spatial temperature and pressure distribution. The initial temperature distribution is generated by simulation of a system with effectively no groundwater flow. For each model with a different terrain shape (i.e. models with different top surface shapes) or a different top thermal boundary condition (e.g. water bodies), the model is first run for 100,000 years with 50-year time-steps with a horizontal and vertical permeability set to a value of nearly zero, 10^{-40} m^2. In these pre-simulations, the starting temperature everywhere in the subsurface and in the air is 2 °C; then air temperature cools linearly over 1,600 years to −6 °C. After 1,600 years, the air temperature is held constant at −6 °C. Although steady-state heat conduction conditions in a cross section with fixed thermal conductivity would occur relatively quickly, when there is freeze/thaw, the vertical temperature distribution changes over a longer time due to the changing amount and position of ground ice, because this also alters the spatial distribution of thermal conductivity. By an elapsed time of 100,000 years, the temperature and permafrost distribution is at or near equilibrium for models of all terrain shapes and top thermal boundary conditions. This equilibrium distribution of temperature provides the initial permafrost distribution for models using each terrain shape, according to the function that specifies ice fraction as a function of temperature. One additional case of initial conditions, generated in the same way as described in the preceding, is assessed with an initially steady temperature of −3 °C, rather than −6 °C.

Subsequently, for each case considered and for each warming simulation, this equilibrium conductive temperature and permafrost distribution is used for calculating the initial pressure distribution for the warming simulation. The initial pressure distribution simulation uses the actual permeability for the case under consideration (not the near-zero permeability). Steady-state pressure conditions are simulated in this second pre-simulation, providing the initial pressure distribution that is used together with the conductive temperature distribution as a complete self-consistent set of initial conditions for the main warming simulation.

Results and discussion

Advection-influenced vs. conduction-only thawing

The divergent evolutions of permafrost thawing during climate warming in conduction-only and advection-influenced hydrogeologic systems are described in the following in reference to results displayed in Fig. 3. In this simulation analysis, the air temperature warms from −6 to 0 °C during the first 600 years (with no seasonal variation). A hydrogeologic reference case is selected that hosts local and larger-scale nested groundwater systems in the ice-free model domain of a stratified silty-sand fabric. This system has a horizontal and vertical permeability of 10^{-12} and 10^{-13} m^2 (approximately equivalent to hydraulic conductivities of 10^{-5} and 10^{-6} m/s respectively). This case has sufficient groundwater flow to impact the thaw process and is thus termed, 'advection-influenced' thaw because heat conduction also plays a role. The advection-influenced thaw rate and pattern are compared with the case in which there is no groundwater flow, termed 'conduction-only' thaw. In the latter case, permeabilities are set to 10^{-40} m^2, effectively inhibiting groundwater flow in the model.

Initial permafrost distribution

Initially, there is a uniform layer of continuous permafrost from the ground surface downwards, ranging approximately in thickness from 220 m below valleys to 300 m below hilltops, with a mildly undulating bottom (this initial condition is shown at the top of Fig. 3, ice saturation at −600 years). This pattern is a product of the way the initial distribution was generated, dependent on a purely conductive temperature distribution in a uniform hydrogeologic system, as explained previously. Because a low air temperature of −6 °C is fixed at the undulating top of the domain in order to provide conditions that will generate permafrost, the vertical temperature distribution varies naturally throughout the subsurface domain in a manner that keeps the vertical heat flux nearly constant at the value imposed at the bottom horizontal boundary. Thus, the lower freeze limit (0 °C) penetrates to lower elevation below valley bottoms than below hilltops.

Conduction-only thawing

The increasing air temperature reaches 0 °C at time '0 years' in Fig. 3. With only heat conduction and linear air-temperature warming, thawing and loss of ice volume from the initial permafrost layer occurs mostly at its upper surface, with an ice-free zone of nearly uniform thickness that is parallel to the land surface, developing above the residual permafrost. This uniformity causes breakthrough to first occur below valley bottoms (after approx. 700 years) where initial permafrost thickness was thinnest.

DOI 10.1007/s10040-012-0942-3

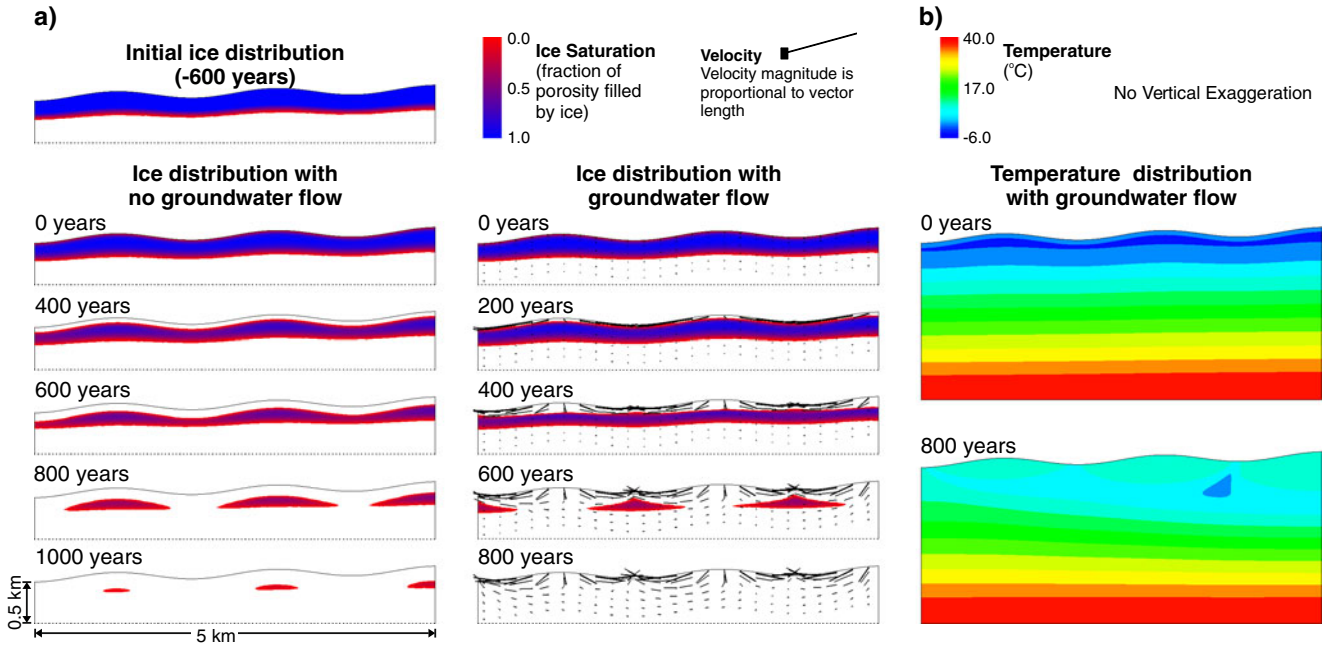

Fig. 3 Comparison of conduction-dominated and advection-influenced permafrost thaw during climate warming showing the permafrost distribution and groundwater flow field in the uppermost 0.5 km of the 2-km-deep model domain (**a**) and showing temperature distribution in entire model domain (**b**). Horizontal permeability, 10^{-12} m^2; vertical anisotropy, 10

Residual permafrost bodies survive longest below hilltops. Should the initial permafrost layer have been of uniform thickness, it would disappear almost simultaneously below hilltops and valleys. It takes more than 1,100 years (after mean annual air temperature reaches 0 °C) for the permafrost to completely disappear.

Advection-influenced thawing

In the 600 years before mean annual air temperature reaches 0 °C, permafrost exists at the ground surface, effectively impeding all groundwater flow (permeability of frozen ground in this case is 10^{-18} m^2, approx. 10^{-11} m/s). The nearly impermeable continuous frozen layer also effectively stops topographic forces from generating flow in the unfrozen zone below the permafrost. Thus, thawing during this period occurs exactly as in the conduction-only case. Figure 3b at 0 years, shows the temperature distribution just before the development of a supra-permafrost thawed zone. Once the air temperature exceeds 0 °C, a permanent zone of thawed ground develops below the land surface, initially parallel to the land surface, as in the conduction-dominated case. However, by 200 years after the start of thaw (see Fig. 3, 200 years), significant groundwater flow in the thin supra-permafrost thawed zone has begun, preferentially thawing permafrost below the hilltops where warm recharge waters enter and flow downward. In contrast to relatively quick thaw below hilltops, the thickness of the thawed zone in valleys increases more slowly because groundwater passing through this area toward low-elevation discharge points has cooled from its relatively warm recharge temperature to near 0 °C as a result of latent heat loss during ice thaw and conductive cooling from colder-deeper ground along its hillside flowpath.

By 400 years, the thickest residual permafrost occurs under the valley bottoms, and the thinnest permafrost occurs below the hilltops. Breakthrough below the hilltops (creating discontinuous permafrost) occurs at about 550 years. Within the discontinuous permafrost, after about 600 years, residual permafrost bodies exist only below valleys, with the thickest and shallowest occurrence of ground ice approximately below the axis of valley centers. These residual permafrost bodies are not symmetric around valley centers, but are skewed downhill (to the left). This is a result of the largest-scale groundwater flow system that results from linearly increasing mean height of the ground surface (to the right). This flow preferentially thaws ground ice on one end of the residual bodies. Residual permafrost bodies thaw primarily at their tops as a result of advection in down-flowing groundwater below hilltops, with a smaller loss at uphill ends due to regional flow, and with least thaw at their bottoms. Permafrost completely disappears by 770 years. After all permafrost thaws, allowing maximum possible deep groundwater flow to be established, an upwelling of geothermally warmed water develops below the primary regional discharge area (the lowest valley in Fig. 3b, 800 years). The nested nature of the open groundwater system is apparent in the flow-vector plot (800 years), with left-right diverging flow below hilltops in the shallower portion of the cross section and right to left regional flow throughout the lower portion of the domain.

Comparison of conductive and advective thawing

In the aforementioned example of advection-influenced thaw, permafrost completely disappears by 770 years. This

DOI 10.1007/s10040-012-0942-3

is about one-third less than the time required for complete permafrost loss in the equivalent conduction-only system (1,100 years). It is notable that the configuration of residual permafrost is quite different between the two cases (Fig. 3). For conduction-only thaw, the residual permafrost bodies are located below valley bottoms; in contrast, for advection-influenced thaw, the residual permafrost bodies are located below hilltops. For conduction-only thaw, the thinnest parts of the permafrost layer thaw through first. For advection-influenced thaw, most thaw occurs where warm recharge water is directed against the permafrost, directly below hilltops; less thaw occurs laterally because groundwater temperature decreases as it flows towards valley discharge points due to the loss of latent heat during thawing that occurred below the hilltops.

The impact of advection on thaw is evaluated by comparing the volume of ground ice for several cases. First, consider the two cases described in the preceding section and an advection-influenced thaw case with ten times higher horizontal and vertical permeability (10^{-11} and 10^{-12} m^2, respectively) than the aforementioned (continuous lines in Fig. 4). Figure 4a shows the total subsurface ice volume as it changes with time for these three cases, and Fig. 4b shows the rate of ice-volume change or equivalently, the thaw rate (smoothed time derivative of the Fig. 4a). Both advective cases exactly follow the evolution of the conduction-only case, from −600 to 0 years, when groundwater flow begins. During this initial conduction-only period, the ice volume decreases gradually from −600 to −200 years as a result of thaw at the base of the permafrost body, due to adjustment of the conductive vertical temperature profile at depth to the increasing air temperature (−6 to −2 °C) during this period. Reduction in ice volume accelerates after −200 years, when the mean annual air temperature reaches −2 °C, the temperature above which the ice saturation within the permafrost body begins to decrease according to the selected ice saturation function (Table 1). After 0 years, the ice volume evolutions for these cases diverge. The rate of thaw for the case with greatest permeability (highest groundwater flow) increases and peaks sooner than does the lower-flow case and reaches a higher thaw rate. The conduction-only thaw rate decreases monotonically after time 0 years. Complete loss of permafrost occurs after 1,100, 770 and 380 years, for the conduction-only, lower flow and higher flow cases, respectively. The case with the highest permeability has unrealistically high regional groundwater flow (due to the fixed water table at the ground surface in the model representation); this case provides an indication of the maximum possible impact that flowing groundwater can have on regional thaw evolution. Taken together, these curves include the full range of possible regional thaw evolutions for this hydrogeologic situation, from slowest possible conduction-only case to the fastest possible high advection case.

Contrary to the expectation that large-scale groundwater flow via through-going taliks would accelerate thaw, thaw rate decreases after the permafrost becomes discontinuous in each case. First breakthrough (the first through-going talik) occurs for the highest flow case at about 250 years, for the lower flow case at about 550 years and for the conduction-only case at about 700 years. Inspection of the thaw rates in Fig. 4 (continuous lines) around these times reveals that the thaw rate decreases not long after the time of breakthrough

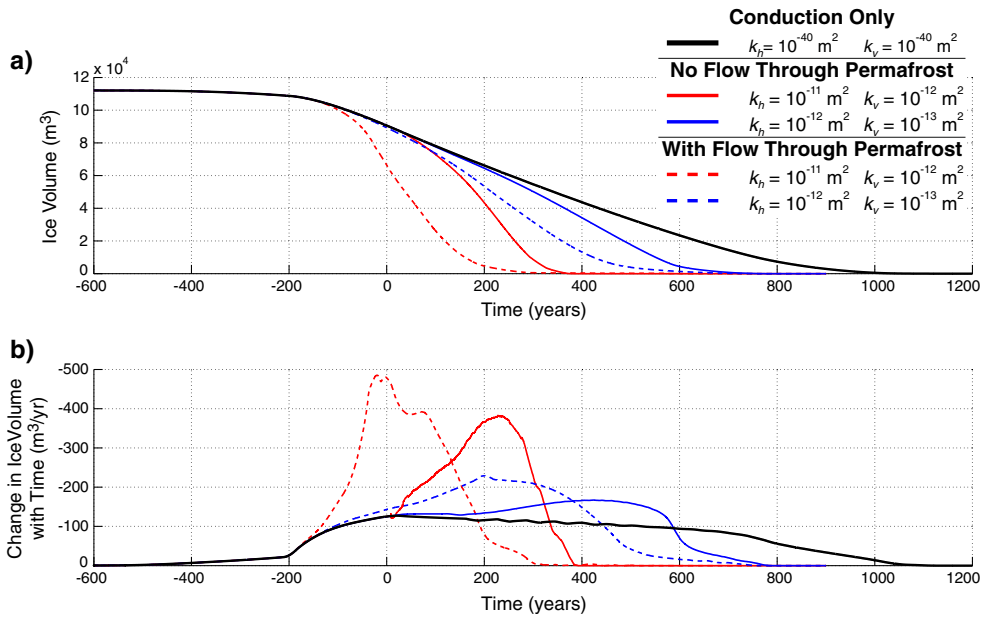

Fig. 4 Comparison of conduction-dominated and advection-influenced permafrost thaw during climate warming, showing evolution of thaw for three situations: conduction-only thaw (permeability $10^{-40} m^2$) and advection-influenced thaw for moderate and high groundwater flow (horizontal permeability 10^{-12} and $10^{-11} m^2$). For advection-influenced cases, results are shown for the situation with only flow around permafrost (i.e. no flow through permafrost) and with flow around and through permafrost. Line color is the same for all cases with the same overall permeability. **a** Shows total ice volume as function of time; **b** shows rate of ice volume change (i.e. thaw rate) as function of time. (Rate is calculated as slope between data points in (**a**) (approx. 30,000 per simulation), then rates undergo a 500-point smoothing.)

DOI 10.1007/s10040-012-0942-3

for both cases (and for the other two cases discussed in the following). There are two possible explanations for this. First, considering that a rate decrease also occurs for the conduction-only case, which has no groundwater flow, the thaw rate decrease for discontinuous permafrost may simply be due to the geometry of the thawing permafrost bodies, rather than to a change in groundwater flow. Alternatively, it may be noted that maximum advection-influenced thaw rates occur while recharging groundwater flows directly towards the permafrost body. This occurs in the downward flowing groundwater below the hilltops before sub-hilltop taliks develop. Once the taliks develop, the residual permafrost bodies have been shaped to conform to the natural groundwater flow directions. Groundwater tends to flow parallel to this streamlined residual permafrost, rather than towards it. This configuration decreases the amount of advective thaw that can occur and thaw rates tend toward a conduction-only rate, once this configuration has developed.

In addition to the aforementioned cases, which demonstrate the impact on thaw evolution of groundwater flowing around (not through) permafrost bodies, the simulations with flow are repeated while allowing groundwater to flow through permafrost (dashed lines in Fig. 4). The relative permeability for this case is a linear function of the ice saturation, ranging from a value of 1 for no ice to a value of 10^{-6} for the maximum ice saturation (0.99). Although little laboratory data are available on which to base this functionality, the linear function selected here likely exaggerates the ease of groundwater flow through frozen media, so results give an indication of maximum impact of this flow on thaw. The results show that permafrost thaw accelerates earlier, in comparison with conduction-only thaw, because some amount of groundwater can flow through the partially frozen permafrost, the amount depending on the ice (conversely, on the liquid water) saturation. The result is that complete loss of permafrost occurs after about 300 years (vs. 380 years for impermeable permafrost) and 750 years (vs. 770 years for impermeable permafrost) for the higher- and lower-permeability cases, respectively. Clearly, the length of time to complete disappearance of permafrost is similar to the respective cases with no groundwater flow through permafrost. However, there are significantly greater losses of permafrost during the early thaw period when groundwater flows through permafrost. For the lower permeability case, loss of 50 % of the initial permafrost volume with flow through permafrost occurs in two thirds of the time required with impermeable permafrost. For the high permeability case, 50 % loss occurs in only 15 % of the time required for impermeable permafrost (23 years vs. 163 years). Late in thaw evolution, the thaw rate with flow through permafrost decreases significantly (when residual ice volume is 10 % and less); this decrease is greater than that for impermeable permafrost, causing ultimate total thaw times to become similar.

Effect of permeability and anisotropy

For given landforms with particular hydraulic driving forces for groundwater flow, the magnitudes of fluid flux and potential advective heat transport are dependent on the permeability of the geologic fabric, making permeability an important control on thawing of ground ice. Thawing of permafrost in the 'Tothian hills' is evaluated via simulation for a variety of geologic fabrics expressed as a range of horizontal permeability values for a fixed vertical anisotropy (horizontal permeability/vertical permeability) and as a range of anisotropy values. Results are shown in Fig. 5a. For a fixed vertical anisotropy value of 10, time to complete loss of permafrost ranges from 770 to 1,107 years. The greatest complete thaw time occurs for the case of conduction-only thaw (line in plot at 1,107 years), but this total thaw time is equivalent to the elapsed times for relatively low horizontal permeabilities of 10^{-15} and 10^{-14} m^2 (approx. 10^{-8} and 10^{-9} m/s), values similar to that of silt, loess or clay. The lowest times occur for the case with the highest horizontal permeability of 10^{-12} m^2 (approx. 10^{-5} m/s), a value similar to that of silty sand. Advection-influenced thaw is indicated by thaw times that are lower than for the case of only conduction; this occurs for horizontal permeability values greater than 10^{-14} m^2 (approx. 10^{-7} m/s), wherein increasing permeability by a factor of ten (and thereby increasing flow by a factor of ten) reduces thaw time by about 15 % over the range considered.

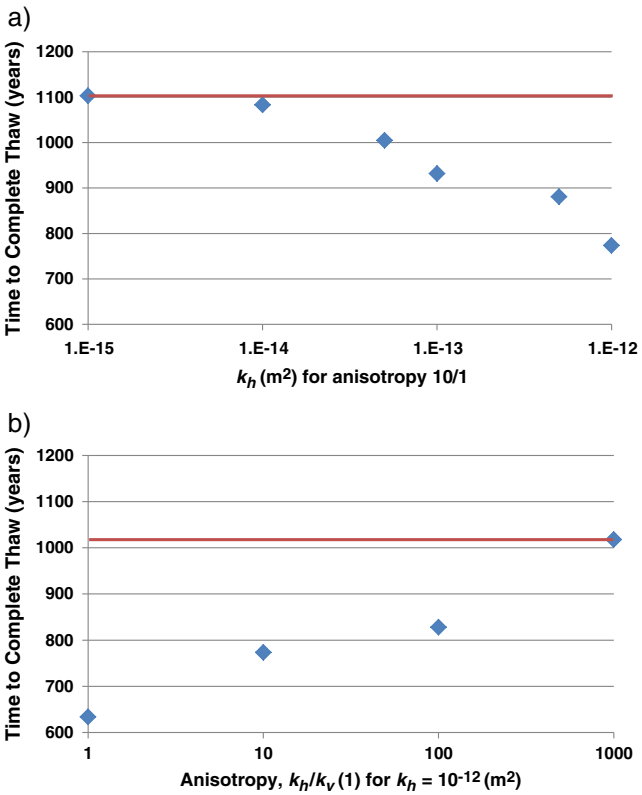

Fig. 5 Time required for complete loss of permafrost, starting with initially continuous permafrost 200 to 300 m in thickness with a low climate-warming rate of 1 °C/100 yr. Impact of: **a** overall permeability and **b** vertical anisotropy in permeability. Time is measured from year when air temperature reaches 0 °C (starting at −6 °C). The *red lines* (at 1,107 years and 1,018 years) shows time required for total thaw in the (**a**) conduction-only and (**b**) high-anistropy situations

DOI 10.1007/s10040-012-0942-3

For the situation with a horizontal permeability of 10^{-12}m^2, a series of thaw simulations with vertical permeability ranging from 10^{-12} to 10^{-15}m^2 have vertical anisotropies ranging from isotropic to 1:1,000 (Fig. 5b). Time to complete thaw for the highest anisotropy is slightly less than the conduction dominated case (line in plot at 1,018 years). For the most-vertically permeable case (isotropic), complete thaw time is reduced to about 630 years. The time to complete thaw increases monotonically with increasing anisotropy with about a 20 % decrease in thaw time for each ten-times-lower anisotropy over the range considered.

Effect of heterogeneity in permeability

Impacts on permafrost thaw of two types of permeability heterogeneity in the geologic fabric, simple layers and patchiness, are evaluated (Figs. 6 and 7). Three examples of layered heterogeneity consist of a single coarse sand layer having 100 times greater horizontal and vertical permeability than the background fabric of silty sand (with horizontal and vertical permeabilities of 10^{-12} and 10^{-13} m^2, respectively, as in one case shown in Fig. 4). The high-permeability zone is alternatively located at three depths: (1) near the bottom of the domain (Fig. 6a), (2) just below the initial continuous permafrost layer (Fig. 6b), and (3) at the top of the domain (Fig. 6c). Layer thickness is approximately 50 m for the bottom and top zones and 100 m for the middle zone. Comparison of the thaw evolution and timing from these three situations with initially continuous permafrost reveals that, if the high-permeability zone is located anywhere below the permafrost, it has little or no effect on the thaw process; the bottom and below-permafrost results (Fig. 6a,b) are practically equivalent. High flow in the zone (see Fig. 6b at 700 years) begins only once permafrost becomes discontinuous, and by that time, most thaw has already occurred, so the higher groundwater flux has little impact. A slight decrease in the size of the residual permafrost body at the leftmost edge of the domain is apparent in the below-permafrost situation due to the increased flow in its vicinity. In contrast, a high-permeability zone located at the top of permafrost (Fig. 6c) enhances supra-permafrost groundwater flow, accelerating thawing from the top and causing much earlier breakthrough and complete permafrost disappearance.

An example of a fabric with dipping high- and low-permeability patches is generated using a repetitive function for $\log_{10}$(permeability) (Fig. 7):

$$k(X,Y) = \left(10^{-12}\right)10^{-2sin}\left(\frac{2\pi(Y-250)}{750}\right)cos\left(\frac{2\pi Y}{1000}+\frac{2\pi X}{2500}\right)$$

where k is the permeability [m^2] (horizontal and vertical values are set equal, isotropic), and X and Y are the horizontal and vertical space coordinates [m], respectively. The mean horizontal permeability of the spatial distribution is the same as for the homogeneous 10^{-12}m^2 horizontal permeability case (Fig. 4b) so that thawing in these can be compared. The times to first breakthrough and complete disappearance of permafrost in the patchy heterogeneous case are 200 and 750 years, respectively, and in the homogeneous case are 600 and 770 years, respectively. A through-going talik forms in the heterogeneous case in one third of the time required in the equivalent homogeneous case, but complete loss of permafrost takes about the same amount of time. Inspection of the patterns of residual permafrost (Fig. 7)

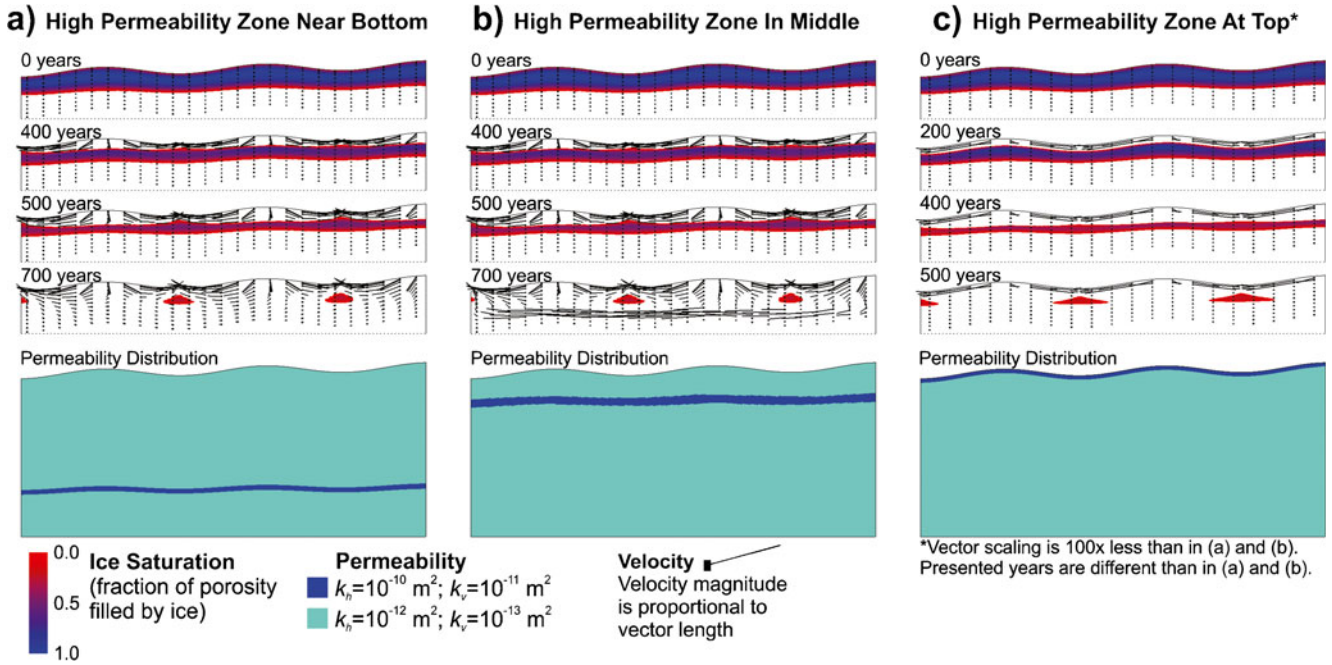

Fig. 6 **a–c** Effect of heterogeneity in permeability on evolution of permafrost thaw patterns: high-permeability layers. Note that the times displayed and the vector scaling vary among panels

DOI 10.1007/s10040-012-0942-3

indicates that thaw occurs preferentially in the high-permeability patches, with much earlier creation of taliks within and near these zones due to higher localized groundwater flow. In contrast, the low-permeability patches preserve permafrost for an extended time due to very low flow and essentially conduction-only conditions within the patch. Permafrost is also preserved in some regions below the low-permeability zone within more-permeable fabric, perhaps as a result of the patch shielding its underside from groundwater flow.

Effect of surface-water bodies

Surface-water bodies such as lakes and streams have a thermal impact on the subsurface region below and immediately surrounding the water body. For most surface-water bodies, particularly for those that do not freeze to the bottom in winter, the subsurface is warmed relative to the surrounding area. This inhibits formation of ground ice, bringing into existence an ice-free zone below the surface-water body. Where the surface-water temperature is high enough and the body wide enough, relative to the thickness of the permafrost layer, the ice-free zone fully penetrates the permafrost, forming a through-going talik. Otherwise, the top of permafrost is merely deepened below the surface-water body. These effects and the impact of groundwater flow on talik development below lakes were first studied by numerical simulation of a single lake by Rowland et al. (2011) and more recently by Wellman et al. (2012). Here, the interaction of surface-water bodies and nested groundwater flow systems are examined in light of climate warming on a relatively large spatial scale, rather than on a local scale.

The 'Tothian hills' hydrogeologic system is simulated with a surface-water body at the bottom of one or more valleys. The surface-water bodies are here referred to as 'lakes'; however, considering the 2D geometry of the simulation, these more rigorously represent streams or rivers extending perpendicular to the modeled cross section, parallel to the axis of the valleys. The possible middle and upper lakes are 400 m across and the lake in the bottom valley is 200 m across. The lakes are modeled as existing above a thermal boundary layer having the same parameterization as on land (e.g. Fig. 1; Table 1), except that the lake bottom has a constant specified temperature of 2 °C and the specified pressure values at lake bottoms are assigned hydrostatic pressure depending on the local depth of the lake, which varies across the lake. The water-level elevations of the three (possible) lakes (from bottom to top) are 1,963.5, 1,999.6, and

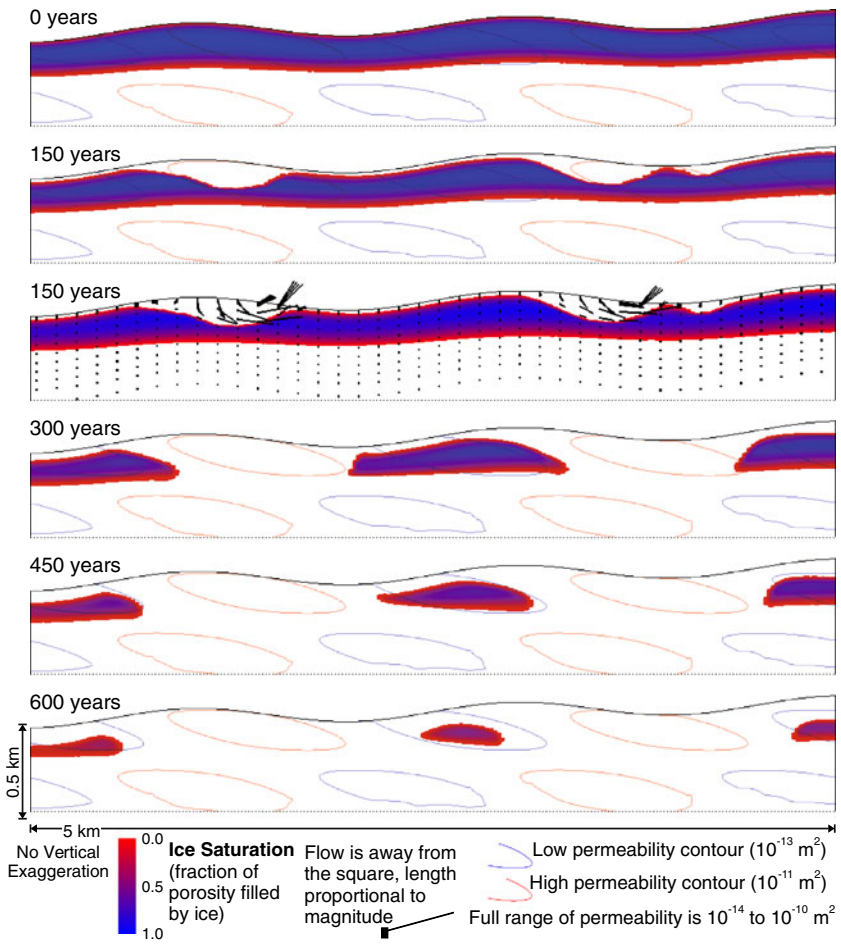

Fig. 7 Effect of heterogeneity in permeability on evolution of permafrost thaw pattern: example with high- and low-permeability patches. The sinusoidal log10 permeability function is given in the text. Vectors delineating the flow field are illustrated for the 150-year result

DOI 10.1007/s10040-012-0942-3

2,039.7 m and the depths of the lakes (from bottom to top) are 13.5, 9.0, and 10.0 m. The horizontal and vertical permeabilities for the lake simulations have the same values as for the case shown in Fig. 4b, 10^{-12} and 10^{-13} m^2. Initial conditions for the lake simulations were created in the same manner as for all simulations in this study, but with one or more lakes and their special boundary conditions on the top surface of the domain. Initial conditions for the lake examples are shown in Fig. 8 (time 0 years). Initial regional permafrost distribution in this case is qualitatively similar to those interpreted from airborne electromagnetic measurements in Yukon Flats, Alaska (Minsley et al. 2012), where there is a through-going talik below most large lakes and streams. However, topographic shape fluctuation in Yukon Flats is much less than in the present examples.

Simulated thaw evolutions with surface-water bodies in different valleys are compared in Fig. 8, and these may all be compared with the equivalent hydrogeologic situation without surface water (Fig. 4b). One result of a lake is the absence of an initial permafrost layer below its valley. Thus, for a sub-lake valley, there will be no long-lasting residual permafrost, as occurs below a lake-free valley when all other permafrost has thawed. Times for total thaw should thereby be reduced. This is borne out by the results, in which total thaw occurs by 600 years or 700 years, depending on the number of lakes, in comparison with total thaw time of 770 years for the no-lake situation. Further, it might be expected that when there are two or more lakes with through-going taliks, some regional groundwater flow occurs even at the beginning of the time period, shortening thaw times due to advection. In this light, it may be noted that the cases with a single lake experience thaw (complete in about 700 years) in a manner similar to the no-lake case, because no regional flow occurs until breakthrough in an additional location. Note in Fig. 8 (clearest at early times) that flow enters higher lakes, passes laterally downhill below permafrost bodies, and discharges to lower lakes. This accelerates thaw somewhat, with complete thaw occurring by 600 years. However, despite the contribution of large-scale deep groundwater flow, the primary thaw mechanism in cases with surface water remains heat advection in the downward flow below hilltops. (One minor complication is that the modeled 2 °C surface-water bodies tend to warm the subsurface while mean yearly air temperature is below 2 °C, but these cool the subsurface after climate warming raises mean yearly air temperature above 2 °C.)

Effect of topographic roughness

Another control on the rate and pattern of permafrost thaw is the fluctuation in topographic (or water table) shape, which drives local and larger-scale groundwater flow. Investigation of some basic variations in the shape of the top boundary allows some insight to be developed. Recall that the shape of the 'Tothian hills' consists of a linear hillslope with an added sinusoidal fluctuation. In this analysis, the amplitude and wavelength of the sinusoidal fluctuation is varied in a few cases, keeping the linear slope the same as in the reference case (amplitude=50 m, wavelength=2,000 m): constant slope with no hills (amplitude=0), hills of double height (amplitude=100 m), hills with double width (wavelength=4,000 m), and hills with half width (wavelength=1,000 m).

Results of these simulations indicate that groundwater flow and the hill shape are both controls on the time required to thaw all permafrost, and that hill shape and groundwater flow magnitude are correlated. To clarify the relation, a 'potential groundwater flow' (PGF) can be defined, which is the total amount of groundwater recharge that would occur in the ice-free situation for a system with any topographic shape, assuming that the water table follows the ground surface. Further, the 'potential groundwater flow due to roughness' (PGFR) is the additional amount of groundwater recharge that occurs in an ice-free situation as a result of the waviness of the topography. For the simulations considered, PGFR has been calculated as the total groundwater recharge for a case with hills minus the groundwater recharge for the no-hill case (with linear hills only). Finally, a measure of the topographic roughness, related to the maximum slope of the sinusoidal hills, is defined as a hill 'aspect ratio', AR=(amplitude/wavelength). The following cases are considered: zero amplitude AR=0, reference case AR=0.025, double width AR=0.0125, half width AR=0.05, and, double height AR=0.05.

PGFR is found to depend on only the AR, not on the hill shape that underlies the AR value; PGFR is approximately linearly proportional to AR over the range of roughness considered. For AR=0, PGFR=0. For the highest AR considered, AR=0.05, PGFR is about 10^{0}kg/s for the 1-m-thick cross-sectional domains simulated. (Linear hill recharge with AR=0 is about 10^{-1}kg/s.) Considering recharge to occur over the entire model top, these values are equivalent to standard recharge rates of about 6 m/yr and 60 cm/yr, respectively. The higher rates of recharge for greater ARs, inflate the recharge rate (and groundwater throughflow) beyond what could be expected to be available, but these cases are useful for developing understanding of controls on the physical process of thaw and maximum possible impacts of advection on thaw.

Time for complete loss of permafrost decreases monotonically with both groundwater flow magnitude (for flow greater than about 10^{-2}kg/s, or equivalently, recharge rate about 6 cm/yr) and with hill AR. Time required for complete thaw is shown as a function of hill AR in Fig. 9. As PGFR increases by ten times due to increased topographic AR, total thaw time decreases by about one third.

Effect of climate-warming rate

The evolution of permafrost thaw is compared for two climate-warming rates, +1 °C/100 yr as in previous simulations and +6 °C/100 yr, beginning at an initial air temperature of −6 °C. These warming rates bracket the

DOI 10.1007/s10040-012-0942-3

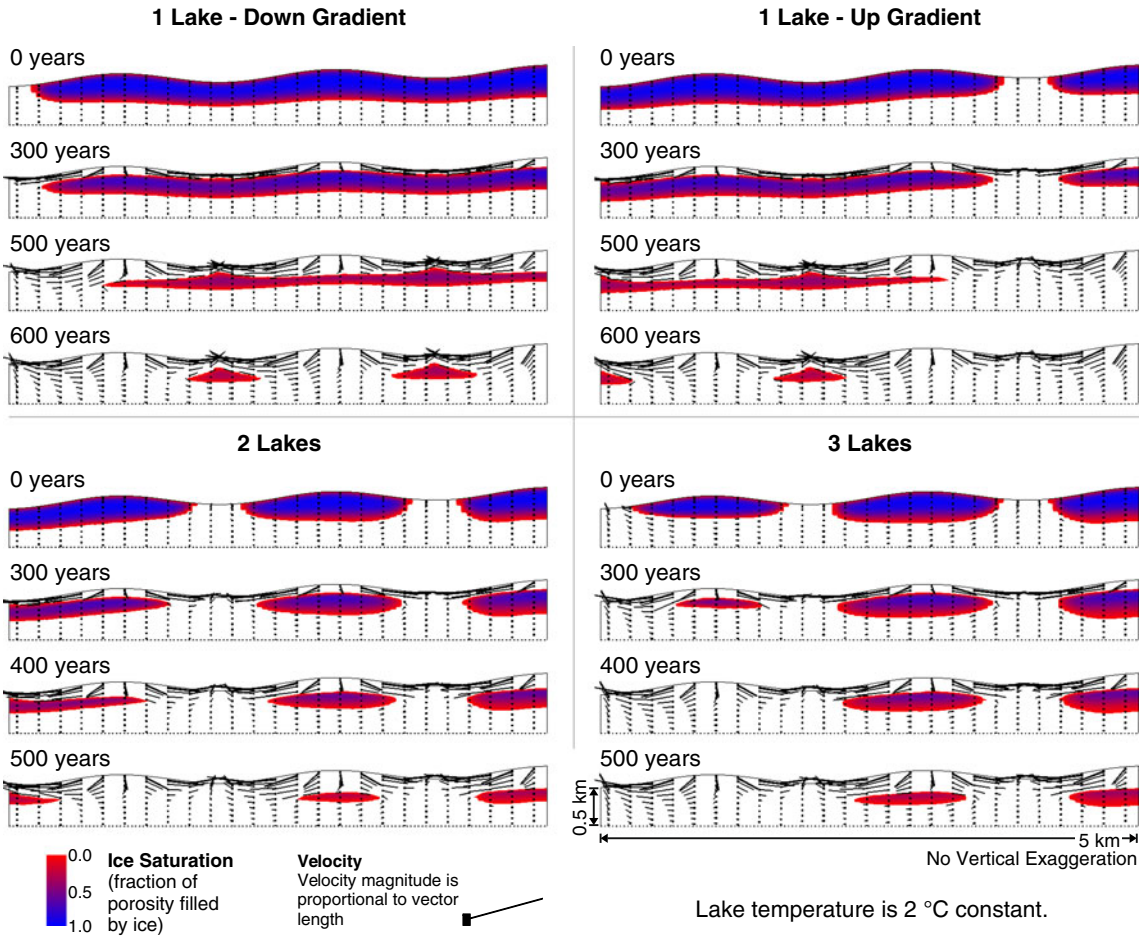

Fig. 8 Effect of surface-water bodies (rivers, lakes) on evolution of permafrost thaw patterns for situation with moderate groundwater flow (horizontal and vertical permeabilities, 10^{-12} and 10^{-13} m^2). Note that the displayed times are different in the *upper* and *lower panels*

range of current IPCC (2007) warming projections. Evolutions are compared for conduction-only and two advection-influenced situations (for the lower permeability case; i.e. horizontal permeability 10^{-12} m^2, anisotropy 10), which either disallow or allow groundwater flow through permafrost.

Simulated times for total thaw under the 1 and 6 °C/100 yr warming rates are respectively: 1,100 and 700 years for conduction-only, and 770 and 500 years for the advection-influenced case. The relations between conduction-only thaw and advection-influenced thaw are illustrated in Fig. 10 (continuous black lines 1 °C/100 yr, continuous red lines 6 °C/100 yr), which shows total ice volume evolution for these cases. The 6 °C/100 yr warming rate results begin at −100 years in Fig. 10 because times are adjusted to be zero when air temperature reaches 0 °C (starting at −6 °C). This higher warming rate reduces time required for complete thaw to two thirds that of the lower warming rate for the conduction-only and advection-influenced systems for the case with no groundwater flowing through permafrost. For both low and high warming rates, increasing potential groundwater flow by 10 times (i.e. increasing permeability by ten times; results not shown here) decreases total thaw time to 40–50 % (from 770 to 380 years and from 500 to 200 years). Time required for complete thaw relative to conduction-only thaw is about 30 % for higher groundwater flow and 70 % for lower groundwater flow, irrespective of the climate-

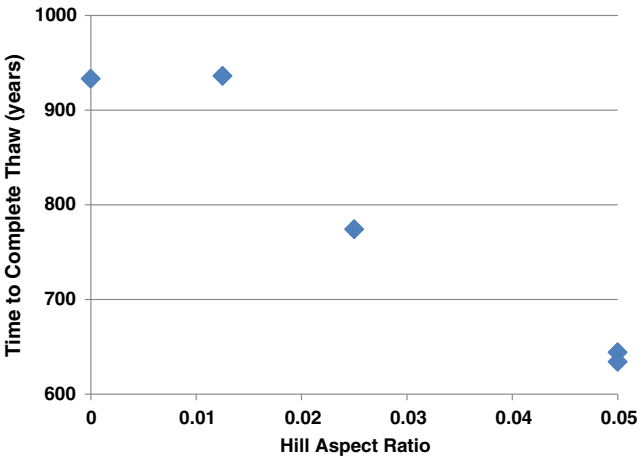

Fig. 9 Impact of topography on time required for complete loss of permafrost, starting with initially continuous permafrost 200–300 m in thickness with a low climate-warming rate of *1 °C/100 yr* for situation with moderate groundwater flow (horizontal permeability 10^{-12} m^2, vertical anisotropy 10). Hill aspect ratio is ratio of topographic amplitude to wavelength. Time is measured from year when air temperature reaches 0 °C (starting at −6 °C)

DOI 10.1007/s10040-012-0942-3

warming rate. A higher warming rate combined with higher groundwater flow decreases the time to complete thaw more than for lower groundwater flow, implying that flow-thaw feedback has a non-linear impact on thaw evolution for warmer air temperature and recharge water. For the situation with groundwater flow through permafrost with 6 °C/100 yr warming (Figure 10, dashed black line 1 °C/100 yr, dashed red line 6 °C/100 yr), complete loss of permafrost occurs in two thirds of the time required for conduction-only thaw. In this case, although flow through permafrost speeds thaw somewhat, the impact is not as great as for the slower rate of climate warming.

Effect of initial permafrost temperature

All of the cases considered in the previous begin with cold permafrost, several degrees C below the temperature at which thaw can occur. The impact of initially warmer permafrost is here evaluated for the case where the initial air temperature is −3 °C, for which even the lowest temperature in the subsurface (−3 °C) is only 1 °C below the temperature at which thaw can occur. In this case, the continuous initial permafrost layer is only about 110 m thick (because the geothermal gradient is fixed) and the total initial ice volume is much lower than in the colder cases. Figure 10 (continuous blue lines) shows that nearly half of the ice volume is lost due to primarily conductive thaw from above by the time groundwater begins to flow (at 0 years). A greater fraction of the initial ice volume is lost by conductive thaw for the case of warmer-thinner permafrost, than for colder-thicker permafrost. For the case of conduction only, complete permafrost loss occurs at 375 years, while groundwater flow (lower permeability case) shortens this time to 250 years, a speed-up of one third. Conversely, conductive thaw takes 50 % longer than advection-dominated thaw for complete loss of permafrost.

Groundwater flowing through warmer-thinner permafrost, according to the linear relative permeability function, described earlier, has less impact on thaw than for colder-thicker permafrost. Figure 10 (dashed blue line) shows ice volume evolution for this case with the +1 °C/100 yr climate-warming rate. In this case with flow through permafrost, a peculiar phenomenon occurs in the simulations—the permafrost body migrates in the subsurface. Flow begins early during warming, wherever permafrost temperature is above −2 °C. Permafrost is lost where groundwater enters the permafrost body and where heat conduction from above increases permafrost temperature, decreasing ice saturation according to the ice saturation function assumed for modeling. Groundwater that flows through the permafrost exits at the downstream edge of the permafrost body—but the temperature of the groundwater exiting is below 0 °C. This water is 'supercooled' as a result of the model assumption that ground ice saturation increases as temperature decreases below zero; thus, the temperature of all liquid water within the permafrost body is sub-zero. Where this groundwater exits the permafrost body, it cools the unfrozen aquifer fabric and forms new permafrost, actually increasing

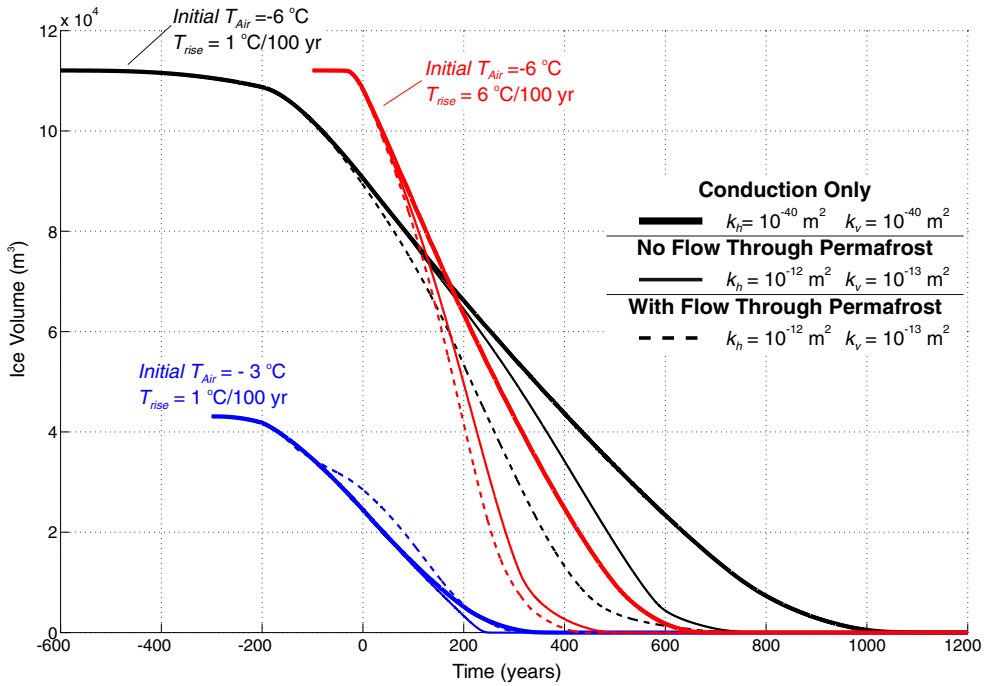

Fig. 10 Comparison of permafrost thaw evolutions for variations in climate-warming rate and initial permafrost state. Total ice volume is shown as a function of time. Cases shown in *black* and *red*: Initially colder-thicker permafrost with low (*1 °C/100 yr*) and high (*6 °C/100 yr*) rates of climate warming comparing conduction-only and advection-influenced (with moderate groundwater flow, horizontal permeability 10^{-12}m^2, vertical anisotropy 10) systems. Case shown in *blue*: Initially warmer-thinner permafrost with low rate of climate warming (1 °C/100 yr) comparing conduction-only and advection-influenced (with moderate groundwater flow, horizontal permeability 10^{-12} m^2, vertical anisotropy 10) systems. *Dashed lines* are for cases that include flow through permafrost. Time is measured from year when air temperature reaches 0 °C for each case

DOI 10.1007/s10040-012-0942-3

the local volume of ice. As a result, the simulated permafrost body slowly migrates in the groundwater-flow direction, as it thaws on the upstream edge and expands on the downstream edge. The result of this process can be seen where the ice volume line crosses and exceeds the conduction-only line in Fig. 10. It is not known whether this is a real phenomenon in the subsurface, or only a figment of the model setup.

Effect of seasonal air-temperature fluctuation

Simulations with a sinusoidal seasonal air temperature fluctuation for a range of amplitudes (±5 , ±10 , ±15 , ±20 °C) superimposed on the linear warming trend of 1 °C/100 yr demonstrate that seasonal air temperature fluctuations have minor impact on regional-scale permafrost total thaw times, but seasonal fluctuations do enhance early thaw rates. Example evolutions of ice volume for the lower flow situation (horizontal permeability 10^{-12}m^2 with anisotropy 10) are shown in Fig. 11 for no yearly fluctuation and for yearly fluctuations with amplitude ±10 and ±20 °C. Although times for total regional thaw are not sensitive to seasonal fluctuations, some impacts on thaw evolution of seasonal fluctuations are apparent in the results and effects are not simple, as discussed in the following. (Here, fractions of initial ice volume are plotted because initial ice volumes are not exactly the same for these situations; the 10 and 20 °C simulations required a finer mesh, and thus had a slightly different starting volume).

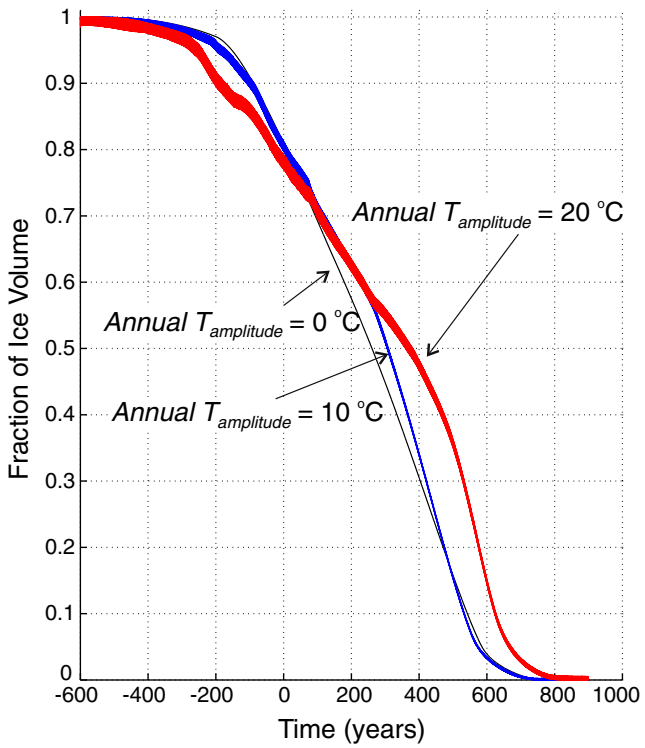

Fig. 11 Comparison of permafrost thaw evolutions for different amplitudes of yearly air temperature fluctuation (*±0 °C*, *±10 °C*, *±20 °C*) with a low rate of climate warming (1 °C/100 yr) for an advection-influenced system with moderate groundwater flow (horizontal permeability 10^{-12}m^2, vertical anisotropy 10) and with no flow through permafrost. The fraction of initial ice volume is shown as a function of time, where the fraction is the ratio of current total residual ice volume to the initial ice volume. Time is measured from the year when mean yearly air temperature reaches 0 °C (starting at −6 °C)

Depending on the amplitude, summer thaw occurs even at the beginning of the simulation. For example, with ±20 °C amplitude, the summer maximum air temperature is 14 °C at simulation starting time −600 years when the yearly mean air temperature is −6 °C. Conversely, there can be winter freezing even after the mean yearly air temperature reaches 0 °C. For example, with ±20 °C amplitude, winter freezing occurs for the following 2,000 years, well beyond the total time simulated. Yearly freeze-thaw changes the total ice volume on a seasonal basis, as indicated by width of the ice-volume band in Fig. 11, which is thicker early and thinner later in the time period simulated. Each apparently solid band is actually a line that oscillates up and down yearly at too fine a scale to appear distinct in the figure. Permanent thaw, significant loss of permafrost volume, begins earlier when there are greater yearly temperature fluctuations (comparing times when the bands first diverge from the no-amplitude case in Fig. 11), for the case of 20 °C amplitude, at about −300 years (i.e. 300 years before the mean yearly temperature reaches 0 °C). This situation has 75 % more permanent ice loss at −200 years than for conduction-only thaw, implying that early time permafrost degradation is significantly increased by seasonal temperature fluctuation, perhaps as a result of enhanced supra-permafrost groundwater flow.

Times to complete disappearance of permafrost decrease only slightly (−30 years) for low amplitude and increase slightly (+45 years) for higher amplitude, relative to the situation with no seasonal fluctuation. The early thaw initiation and non-monotonic relation of amplitude and total thaw time are likely due to non-linear interaction of annual freezing and thawing with groundwater flow. These effects are of importance to local (rather than regional) thaw patterns and evolution (for example, as evaluated by Wellman et al. 2012).

Conclusions

This generic simulation study provides an initial evaluation of some of the key controls on evolution of permafrost thaw during climate warming in a nested groundwater system. Simulations represent the interactive behavior of groundwater flow and ground ice formation and thaw, and results obtained here are generally applicable to understanding of cold-regions hydrologic processes. Controls considered include topographic roughness, ease of groundwater flow external to and within permafrost bodies (overall permeability, vertical anisotropy and relative permeability), climate-warming rate and amplitude of yearly air temperature fluctuations, heterogeneity in geologic structure, location of surface-water bodies, and, initial permafrost temperature.

Even if permafrost itself is relatively impermeable and hosts negligible flow of groundwater through any regions of frozen ground, when such permafrost thaws from above, taliks (ice-free regions in otherwise continuous

DOI 10.1007/s10040-012-0942-3

permafrost) allow groundwater to first flow laterally above the permafrost, then to flow downward below recharge areas as taliks deepen, and once taliks fully penetrate the permafrost, allow groundwater to pass vertically through the permafrost layer. These unfrozen pathways in frozen ground allow heat to be advectively transported at greater rate than by conduction alone. Once advective pathways open in permafrost, geothermally warmed water from below or relatively warm groundwater recharge from above can migrate through the subsurface, expanding the talik network by accelerating thawing along the periphery of residual permafrost. This thaw-flow feedback accelerates thawing especially at early stages of thaw. Should permafrost also host groundwater flow internally within frozen regions, thaw rates, especially early during warming periods, are further enhanced by the additional flow that reduces ice saturations within the permafrost body.

Results of simulation analysis demonstrate that where groundwater flows readily in unfrozen ground surrounding permafrost bodies, it is an important control on the temporal and spatial evolution of permafrost during periods of thaw. Systems with groundwater flow will experience accelerated rates of permafrost degradation overall, and regional patterns of residual permafrost can be very different in conduction-only and advection-influenced groundwater systems. Conversely, where groundwater flow in unfrozen ground is minimal such as where the subsurface has very low permeability inhibiting flow, where the subsurface is highly stratified with low vertical permeability, or where ground ice is spatially continuous over large areas (blocking recharge), heat conduction is the primary thaw process affecting permafrost evolution during climate warming.

The greatest impact of groundwater flow on permafrost evolution occurs below recharge areas where vertically flowing relatively warm recharge is directed toward permafrost bodies. Taliks form preferentially below such recharge areas (hilltops in the present analysis). Subsequently, the recharging groundwater is cooled due to latent heat loss and conduction during thaw and then it flows laterally towards discharge areas (generally parallel to permafrost bodies). As a result, in these discharge areas, advectively influenced thaw is significantly reduced, allowing permafrost to remain longer during climate warming. In cases where low-elevation areas (valleys in the present analysis) contain perennially unfrozen surface-water bodies, taliks already exist so there can be no long-lasting residual permafrost there. In this case, residual permafrost lasts longest below recharge areas, but the time required for total loss of permafrost is less than for the case with no surface water in valleys. Local groundwater flow conditions within the nested flow system control the thaw process during climate warming. Permafrost below local recharge areas will experience greater thaw rates than discharge areas, no matter where these are located within the nested groundwater system. High permeability zones within or near recharge areas also facilitate local thaw acceleration.

Sub-permafrost groundwater flow (recharging through up-gradient taliks and discharging through down-gradient taliks) has less impact on evolution of regional permafrost thaw in comparison with supra-permafrost flow, especially within recharge areas. Energy required for thaw must come from either warm surface recharge or from deep geothermally warmed groundwater. The surface recharge cools while it travels through the subsurface as it loses heat due to conduction and as it thaws ground ice. Thus, after some subsurface travel distance and after passing downward through an open talik to the sub-permafrost aquifer, the ability of recharge waters to thaw permafrost is greatly reduced, making sub-permafrost flow less effective in regional permafrost thaw. Geothermally warmed groundwater discharges only in particular locations in a nested groundwater system depending on natural convection, on regional topographic hydraulic gradients and on hydrogeologic structure. Where it reaches the bottom of permafrost, it may cause thinner permafrost or through-going taliks or widening of existing taliks. However, due to the low magnitude of most deep groundwater movement, geothermally mediated thaw is likely slow compared to the thaw rate imposed by supra-permafrost flow. Despite this expectation that sub-permafrost groundwater flow has only a minor impact on regional permafrost thaw evolution, it can play a more-important role in developing thaw locally such as within a lake talik (Wellman et al. 2012). On the local scale, sub-permafrost flow can interact more dynamically with supra-permafrost flow, surface water and zones of ground ice with measurable impact on local processes.

Climate-warming rates considered bracket the IPCC (2007) lowest and highest predicted rates. Times (measured after the mean annual air temperature reaches 0 °C, starting at −6 °C) for total thaw of an initially continuous relatively cold permafrost layer of 200 to 300 m thickness determined from simulations with a low rate of climate warming of 1 °C/100 yr, range from about 1,100 years for conduction-only systems to 750 years for nested groundwater systems with moderate flow, to a minimum of 380 years for very high groundwater flow. With a high rate of climate warming of 6 °C/100 yr, total thaw of an initially continuous relatively cold permafrost layer ranges from 700 years for conduction-only systems to a minimum of 200 years for systems with very high flow. If the permafrost layer is initially discontinuous, with through-going taliks initially below valley surface-water bodies, time for total thaw may be further reduced by about 100 years. For relatively warm continuous permafrost (close to its thaw temperature), heat conduction during early stages of climate warming can result in significant loss of ice volume, but once groundwater can flow in taliks, thaw accelerates relative to locations where conduction dominates, resulting in reduction of conductive total thaw time by one third in one case considered here (250 years with flow vs. 375 years without flow). Note that the thaw time reductions resulting from groundwater flow reported in this work are maximum estimates for each case considered. This is due to the simplifying model assumption of a constant water-table elevation coincident with the land-surface topography,

 DOI 10.1007/s10040-012-0942-3

which augments simulated groundwater recharge and flow. Actual thaw times in most areas with groundwater flow should be greater than the values reported here, although in locales where groundwater flow is particularly enhanced due to hydrogeologic conditions (such as in the high permeability regions of a heterogeneous hydrogeologic structure), actual thaw rates may approach the maximum values provided here.

Walvoord et al. (2012) have found for the Yukon River Basin (Alaska, USA) that large changes in proportions and quantities of supra-permafrost and sub-permafrost groundwater discharging to streams may occur when areal permafrost extent decreases during climate warming from continuous permafrost to less than 90 % of the area underlain by permafrost. In terms of the current study, this means that early stages of permafrost degradation could have the greatest impact on hydrologic systems and their dependent ecosystems. The earliest stage of permafrost thaw is here found to be controlled by heat conduction primarily from warming temperatures at the ground surface. Thereafter, in settings where groundwater can flow readily in unfrozen ground, there are two types of groundwater flow that then enhance thaw rates: flow around the periphery of permafrost bodies, and flow through permafrost bodies. Where taliks have formed in such settings as a result of initial conductive thaw, groundwater flow around permafrost bodies can greatly increase the rate of thaw and can strongly impact the spatial pattern of taliks and residual permafrost. Furthermore, flow through (rather than around) frozen ground within permafrost bodies is found to particularly enhance early stage thaw, perhaps making this an important factor for assessing early permafrost loss during climate warming.

To summarize, this generic basic analysis of nested groundwater systems in cold regions shows that where groundwater flow occurs in areas with permafrost, its action during periods of climate warming can cause significant heat-advection-based increases in rate of thaw and significantly different patterns of residual permafrost, in comparison with cold regions where groundwater flow is small and heat conduction is the major thaw process. Once significant groundwater flow begins in regions with sufficiently high unfrozen permeability, with continued climate warming, relatively cold permafrost layers of a few hundred meters in thickness can completely disappear in only some hundreds of years and relatively warm thinner permafrost layers can disappear even more quickly. Early thaw rate following onset of climate warming is particularly enhanced by groundwater flow, and this is the time when adverse environmental impacts of permafrost loss may be the most severe.

In future work, there is need for deeper simulation analysis of the currently considered factors and of other factors on permafrost evolution, such as insolation and vegetation patterns. Due to the importance of permafrost as a hydrogeologic barrier, the loss of permafrost will have major impacts on cold-regions surface waters, chemical exports, ecology, geomorphology, and human infrastructure. Prediction and possible mitigation of adverse effects in cold regions thus requires improved characterizations of groundwater hydrology, of permafrost distribution and dynamics, and of hydrologic properties of frozen porous media, all of which are currently lacking due to the remoteness of much of the area of concern.

Acknowledgements This project has received support from: Fonds de recherche Nature et technologies, Quebec, McGill University, Canada, US Geological Survey (USGS) National Research Program, USGS Climate and Land Use Change and Water Mission Areas, and grant RC-2111 of the US Government Interagency (DOD, EPA and DOE) Strategic Environmental Research and Development Program (SERDP). This article has greatly benefited from insightful helpful reviews by Michelle Walvoord (USGS), Joel Rowland (LANL), Bryan Travis (LANL) and Larry Hinzman (IARC).

References

Bense VF, Ferguson G, Kooi H (2009) Evolution of shallow groundwater flow systems in areas of degrading permafrost. Geophys Res Lett 36:L22401. doi:10.1029/2009GL039225

Bense VF, Kooi H, Ferguson G, Read T (2012) Permafrost degradation as a control on hydrogeological regime shifts in a warming climate. J Geophys Res 117:F03036. doi:10.1029/2011JF002143

Frampton A, Painter S, Lyon SW, Destouni G (2011) Non-isothermal, three-phase simulations of near-surface flows in a model permafrost system under seasonal variability and climate change. J Hydrol 403(3–4):352–359

Ge S, McKenzie J, Voss C, Wu Q (2011) Exchange of groundwater and surface-water mediated by permafrost response to seasonal and long-term air temperature variation. Geophys Res Lett 38: L14402. doi:10.1029/2011GL047911

IPCC (2007) Contribution of Working Groups I, II and III to the Fourth Assessment Report of the Intergovernmental Panel on Climate Change Core Writing Team. In: Pachauri RK, Reisinger A (eds) IPCC, Geneva, Switzerland

Kane DL, Hinkel KM, Goering DJ, Hinzman LD, Outcalt SI (2001) Non-conductive heat transfer associated with frozen soils. Glob Planet Chang 29:275–292

Kell GS (1967) Precise representation of volume properties of water at one atmosphere. J Chem Eng Data 12(1):66–69

McKenzie JM, Siegel DI, Rosenberry DO, Glaser PH, Voss CI (2006) Heat transport in the Red Lake Bog, Glacial Lake Agassiz Peatlands. Hydrol Process 21(3):369–378

McKenzie JM, Voss CI, Siegel DI (2007) Groundwater flow with energy transport and water–ice phase change: numerical simulations, benchmarks, and application to freezing in peat bogs. Adv Water Resour 30:966–998. doi:10.1016/j.advwatres.2006.08.008

Minsley BJ, Abraham JD, Smith BD, Cannia JC, Voss CI, Jorgenson MT, Walvoord MA, Wylie BK, Anderson L, Ball LB, Deszcz-Pan M, Wellman TP, Ager TA (2012) Airborne electromagnetic imaging of discontinuous permafrost. Geophys Res Lett 39:L02503. doi:10.1029/2011GL050079

Painter SL (2011) Three-phase numerical model of water migration in partially frozen geological media: model formulation, validation, and applications. Comput Geosci 15:69–85

Rowland JC, Travis BJ, Wilson CJ (2011) The role of advective heat transport in talik development beneath lakes and ponds in discontinuous permafrost. Geophys Res Lett 38:L17504. doi:10.1029/2011GL048497

Tilton LW, Taylor JK (1937) Accurate representation of the refractivity and density of distilled water as a function of temperature. J Res Natl Bur Stand 18:205–214

Toth J (1963) A theoretical analysis of groundwater flow in small drainage basins. J Geophys Res 68(16):4795–4812

Voss CI, ProvostAM(2002) SUTRA: a model for saturated-unsaturated, variable-density ground-water flow with solute or energy transport. US Geol Surv Water Resour Invest Rep 02–4231, 250 pp. US Geological Survey, Reston

Walvoord MA, Voss CI, Wellman TP (2012) Influence of permafrost distribution on groundwater flow in the context of climate-driven permafrost thaw: example from Yukon Flats Basin, Alaska, USA. Water Resour Res 48:W07524. doi:10.1029/2011WR011595

Wellman TC, Voss CI, Walvoord MA (2012) Impacts of climate, lake size, and supra- and sub-permafrost groundwater flow on lake-talik evolution, Yukon Flats, Alaska (USA). Hydrogeol J. doi:10040_10.1007/s10040-012-0941-4

White D, Hinzman L, Alessa L, Cassano J, Chambers M, Falkner KK, Francis J, Gutowski B, Holland D, Holmes RM, Huntington H, Kane D, Kliskey A, Lee C, McClelland J, Peterson B, Straneo F, Steele M, Woodgate R, Yang D, Yoshikawa K, Zhang T (2007) The Arctic freshwater system: changes and impacts. J Geophys Res 112:G04S54